Title

A facile strategy for fine-tuning the stability and drug release of stimuli-responsive cross-linked micellar nanoparticles towards precision drug delivery

Journal

Nanoscale, 9(23)

ISSN

2040-3364

Authors

Xiao, Kai
Lin, Tzu-yin
Lam, Kit S
et al.

Publication Date

2017-06-14

DOI

10.1039/c7nr02530k

Peer reviewed

HHS Public Access

Author manuscript

Nanoscale. Author manuscript; available in PMC 2018 June 14.

Published in final edited form as:

Nanoscale. 2017 June 14; 9(23): 7765–7770. doi:10.1039/c7nr02530k.

A facile strategy for fine-tuning the stability and drug release of stimuli-responsive cross-linked micellar nanoparticles towards precision drug delivery

Kai Xiao[a], **Tzu-yin Lin**[b], **Kit S. Lam**[c], and **Yuanpei Li**[c]

[a]National Chengdu Center for Safety Evaluation of Drugs, State Key Laboratory of Biotherapy, Collaborative Innovation Center for Biotherapy, West China Hospital, Sichuan University, Chengdu, 610041, PR China

[b]Department of Internal Medicine, Division of Hematology/Oncology, University of California Davis, Sacramento, CA 95817, USA

[c]Department of Biochemistry and Molecular Medicine, UC Davis Comprehensive Cancer Center, University of California Davis, Sacramento, CA 95817, USA

Abstract

Precision drug delivery has great impact on the application of precision oncology for better patient care. Here we report a facile strategy for fine-tuning the stability, drug release and responsiveness of stimuli-responsive cross-linked nanoparticles towards precision drug delivery. A series of micellar nanoparticles with different levels of intramicellar disulfide crosslinkages could be conveniently produced with a mixed micelle approach. These micellar nanoparticles were all within a size range of 25–40 nm so that they could take full advantage of the enhanced permeability and retention (EPR) effect for tumor-targeted drug delivery. The properties of these nanoparticles such as critical micelle concentration (CMC), stability, drug release and responsiveness to reductive environment could be well correlated to the levels of crosslink (LOC). Compared to the micellar nanoparticles with a LOC at 0% that caused death of animals of two species (mouse and rat) due to the acute toxicity such as hemolysis, the nanoparticles at all other levels of crosslink were much safer to be administered into animals. The *in vitro* antitumor efficacy of micellar nanoparticles crosslinked at lower levels (20% & 50%) were much more effective than that of 100% crosslinked micellar nanoparticles in SKOV-3 ovarian cancer cells.

Graphical Abstract

Correspondence to: Kit S. Lam; Yuanpei Li.

†Electronic Supplementary Information (ESI) available. See DOI: 10.1039/x0x00000x

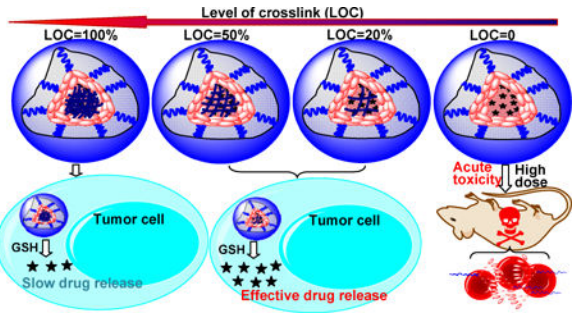

A facile strategy is described to move the field of drug delivery a major step forward towards precision drug delivery.

Introduction

Precision medicine is “an emerging approach for disease treatment and prevention that takes into account individual variability in genes, environment, and lifestyle for each person[1].” The near-term goal is to intensify efforts to apply precision medicine in cancer. It relies on three major approaches including gene sequencing, big data and biomedical analysis to identify best drugs based on their molecular mechanisms specifically for each individual cancer patient. However, many drugs selected for cancer treatment are too toxic for systemic administration. The development of precision drug delivery systems with precisely controlled stability and programmed drug release property has enormous potential to reduce the toxicity of the drugs and enhance their therapeutic efficacy. It will greatly facilitate the application of precision medicine in oncology for better care of cancer patients[2].

Due to their superior biocompatibility, relatively smaller diameter (10–100 nm) and high capacity to encapsulate hydrophobic drugs, micellar nanoparticles are ideal candidates for the development of precision drug delivery systems[2–21]. Furthermore, recent advancement in materials sciences and nanotechnology has led to the creation of a new generation of such nanoparticles called stimuli-responsive cross-linked micellar nanoparticles (SCMNs). These smart SCMNs utilized a stimuli-responsive cross-linking strategy to control the release rate of the drug payloads in different environments (e.g. normal tissue versus tumor microenvironments)[8, 18, 22–25]. SCMNs exhibited minimal premature drug release in blood circulation due to their superior structural stability while they could release their drug payloads upon the stimulation in the local environment of the tumor[24].

The concept of SCMNs appears to be very attractive in terms of reducing the systemic toxicity and increasing the antitumor efficacy. However, in many cases, excessively crosslinked micellar nanoparticles may prevent the drug from releasing to target sites effectively, thus reducing the therapeutic efficacy[26]. While free drug quickly spreads within the tumor tissue, crosslinked nanoparticles, even with a certain type of triggering mechanism, release their content at a relatively slow rate to tumor cells, once they deposit at the target tumor site. This slow release generates a low temporal and spatial concentration gradient of the drug, resulting in non-cytotoxic levels of the drug distal from these particles[27]. Therefore, it is very important to create new drug delivery systems that are

simultaneously resistant to drug leakage in blood and able to rapidly release their drug payloads in tumors to minimize the side-effects and further enhance the therapeutic index.

Recently our group developed two classes of SCMNs for programmable drug delivery. The first class of crosslinked micelle system is called “disulfide crosslinked micelles (DCMs)”. The disulfide crosslinks are cleaved inside the tumor cells under a reductive environment by glutathione (GSH) or on-demand with the administration of N-acetylcysteine (NAC, Mucomyst®)[18, 24, 26, 28–30]. The second crosslinked micelle system is called “boronate crosslinked micelles (BCMs)” [31]. The boronate crosslinks can be cleaved in the acidic tumor extracellular environment and in the acidic cellular compartments upon uptake in target tumor cells, and/or by the administration of mannitol (Osmitrol®) as an on-demand triggering agent.

Here we show that the stability, drug release and responsiveness to reductive environment of DCMs could be further fine-tuned with a mixed micelle approach by varying the ratios of a thiol-free telodendrimer and a thiolated telodendrimer contained four cysteines (Fig.1). Such approach greatly enhanced the *in vitro* antitumor efficacy of DCMs while retained the micellar stability at an appropriate level to prevent the severe acute toxicity caused by the haemolytic nature of non-crosslinked micellar nanoparticles.

Results and discussion

A series of micellar nanoparticles with various levels of intra-micellar disulfide crosslinkage (Fig. 1) could be conveniently prepared by using a mixed micelle approach. It was achieved by adding different ratios of thiol-free telodendrimer (PEG^{5k}-CA_8)[16] and thiolated telodendrimer (PEG^{5k}-Cys_4-L_8-CA_8)[26] into organic solvents such as ethanol, followed by solvent-evaporation, rehydration with aqueous solution and then oxidation with hydrogen peroxide. The completion of oxidation of free thiol groups to form intramicellar disulfide bonds was monitored by quantitative Ellman test as described in our previous study[26].

The level of crosslink (LOC) was defined as the molar ratios of PEG^{5k}-Cys_4-L_8-CA_8 thiolated telodendrimer within the total telodendrimers. The morphology of the micellar nanoparticles at all LOCs was observed to be spherical by a TEM after staining with phosphotungstic acid (Fig. 2). The size of these micellar nanoparticles with LOCs ranging from 0% to 100% analyzed by TEM and DLS were within a range of 22–40 nm (Fig. 2, Table S1). Therefore, by using this mixed micelle approach we created an excellent micellar delivery system with similar sizes to investigate the effect of LOC on the properties of these nanoparticles.

The critical micelle concentration (CMC) is the minimum concentration of polymer required for micelles to form. The CMC is a fundamental parameter to characterize the thermodynamic stability of micelles[32]. Pyrene was used as a hydrophobic fluorescent probe to determine the CMC values of a series of disulfide crosslinked micellar nanoparticles with LOCs at 0%, 10%, 20%, 30%, 50% and 100%. The CMC value of non-crosslinked micellar nanoparticles (LOC = 0%) were 50.1 μg/mL (Fig. 3). At a LOC of 100%, there was 8 times decrease in the value of apparent CMC of micellar nanoparticles (to 6.5 μg/mL) (Fig. 3). The

dramatic decrease in CMC value indicated a significant increase in the thermodynamic stability of the micellar nanoparticles. Furthermore, the CMC value could be fine-tuned by the LOCs of micellar nanoparticles (Fig. 3), indicating the stability of these micellar assemblies were wellregulated based on the LOC.

The stability of micellar nanoparticles with a variety of LOCs were further investigated by the real-time measurements of their particle size in severe micelle-disrupting conditions in the presence of sodium dodecyl sulfate (SDS)[26]. Within 10 seconds, the particle size signal of non-crosslinked micellar nanoparticles (LOC = 0%) immediately disappeared as reported previously[26], reflecting the distinct dynamic associationdissociation property of non-cross-linked micelles. The constant particle size of the DCMs at all levels of crosslink under similar condition over time indicated that such crosslinked micelles remained intact (Fig. 4). The GSH concentration inside cells (~10 mM) is known to be substantially higher than the extracellular level[26]. In the presence of SDS plus the addition of GSH (10mM), the particle size of disulfide crosslinked micelle at all levels of crosslink (LOC= 10% to 100%) remained unchanged for a certain amount of time until it disappeared suddenly (Fig. 4), indicating that rapid dissociation of the micellar nanoparticles did occur when a critical number of sulfide bonds were reduced. Fig. 4 clearly demonstrated that the time-delay dissociation, with the addition of 10 mM of GSH, could be fine-tuned by varying the ratio of PEG^{5k}-Cys_4-L_8-CA_8 thiolated telodendrimer with thiol-free telodendrimer (PEG^{5k}-CA_8) (from 10%–100%). At the tumor site and particularly inside the tumor cells, where the GSH level is high and therefore the dissociation and subsequent drug release is expected to occur based on the levels of disulfide crosslinkages.

We have successfully encapsulated many types of chemotherapeutic drugs into our crosslinked micellar nanoparticles [18, 24, 26, 28–30]. In some clinical situations, these nanoparticle drugs may have to be administrated at high dose if the drug itself is not very effective. Therefore, investigation of the toxicity of the empty nanocarriers at high dose will facilitate the versatile applications of these nanoparticle platforms. The *in vivo* toxicity profiles of micellar nanoparticles with a variety of LOCs were further evaluated in tumor free nude mice and rats via tail vein injection. At a single dose of 200 mg/kg, all the mice in non-crosslinked micellar nanoparticles (LOC = 0%) group showed significant body weight loss, and 1 of 4 mice and 2 of 4 rats died within 1 day post-injection (Table 1). All the mice and rats in these groups treated with a higher dose (400 mg/kg) of non-crosslinked micellar nanoparticles (LOC = 0%) died within 2 hrs postinjection due to acute toxicity (Table 2). Bloody urine was observed for most of the mice and rats, indicating the hemolytic potential caused by non-crosslinked micellar nanoparticles at high dosage. On the contrary, none of the mice and rats treated with crosslinked micellar nanoparticles (LOC ranging from 20 to 100%) were dead at the single dose of 200 or 400 mg/kg (Table 1&2) and no obvious sign of toxicity was observed within two weeks post-injection. This important observation indicated that even with a LOC at 20%, the intramicellar crosslinkages could stabilize the micellar nanoparticles in blood, preventing them from interaction with the red blood cells and therefore avoiding the acute toxicity caused by hemolysis.

As described above, the size of these micellar nanoparticles was all within a size range of 22–40 nm. Due to this relatively smaller size and enhanced stability, the disulfide

crosslinked micellar nanoparticles could take full advantage of the enhanced permeability and retention (EPR) effect for tumortargeted drug delivery. We demonstrated DiD and paclitaxel (PTX) co-loaded micellar nanoparticles at a LOC of 20% and 50% were able to preferentially accumulate in the tumor sites in nude mice bearing SKOV-3 ovarian carcinoma xenograft at 24 hrs post-injection (Fig.5 & Fig. S1, S2). The semiquantitative analysis from *ex vivo* images indicated that accumulation in tumor of both micellar nanoparticles (LOC= 20% and 50%) was 5 and 7 times higher than that in muscle at 24 and 48 hrs post-injection, respectively (Fig. S3).

PTX, an important microtubule stabilizer for cancer treatment, was physically encapsulated into the micellar nanoparticles with a variety of LOCs as a model drug to investigate the release profiles of these particles by using the dialysis method. The particle size of these micellar nanoparticles after drug loading did not change significantly (Table S1). As shown in Fig.6 and Fig. S4 **left panel**, the release of the encapsulated PTX from the crosslinked micellar nanoparticles (LOC = 20%, 50% and 100%) was much slower than that of the non-crosslinked counterparts. For the micellar nanoparticles with LOCs at 20%, 50% and 100%, it was noted that the PTX release was gradually facilitated as the GSH concentration increased up to the intracellular level (10 mM) (Fig.6 and Fig. S4 **right panel**). When GSH was added at the 5 hrs time point, there was a dramatically promoted drug release from the crosslinked micellar nanoparticles (LOC = 20%, 50% and 100%) but not from the non-crosslinked ones (Fig.6 and Fig. S4 **right panel**). Furthermore, the release rate of PTX and responsiveness of these crosslinked micellar nanoparticles could be well-controlled by varying their LOCs (Fig.6 & Fig. S4), providing a tunable drug delivery system for different biological applications towards precision drug delivery.

As demonstrated above, the crosslinked micellar nanoparticles with LOCs at 20%, 25%, 50% and 100% were much safer to be administrated into mice and rats via tail vein compared with their non-crosslinked counterparts. Next, we aimed to determine the LOCs of the micellar nanoparticles that can most effectively kill cancer cells. The *in vitro* anticancer activity of PTX encapsulated micellar nanoparticles (LOC=0%, 20%, 50% & 100%) was evaluated on SKOV-3 ovarian cancer cells. The SKOV-3 cells were incubated with different nanoformulations of PTX for 2 hrs, washed with PBS to remove the extracellular drugs and then further incubated for 22 and 46 hrs (total 24 and 48 hrs) respectively. The PTX loaded micellar nanoparticles with a LOC of 100% was less effective than that with all other LOCs at both time points ($P < 0.05$), which was expected due to the slower drug release from PTXencapsulated nanoparticles both in cell culture media and in cells after their cellular uptake (Fig.7). The PTX loaded micellar nanoparticles with LOCs at 20% and 50% exhibited a similar *in vitro* anticancer efficacy compared to that with a LOC at 0% at 48 hrs (Fig.7). As controlled groups, the corresponding empty micellar nanoparticles at all LOCs under identical total micelle concentration did not show obvious cytotoxicity against SKOV-3 cells (total incubation time: 48 hrs) (Fig. S5). The above result indicated that the relatively lower level of disulfide crosslinkage could be effectively cleaved by intracellular GSH, and facilitated intracellular drug release, which results in enhanced cytotoxicity compared to that crosslinked at 100%.

Conclusions

In this report, we described a facile mixed micelle strategy for fine-tuning the stability, drug release and reductive stimuli responsiveness of disulfide crosslinked micellar nanoparticles. This is an effective approach to greatly enhance the antitumor efficacy of disulfide crosslinked micellar nanoparticles while retaining the micellar stability to minimize the severe acute toxicity. Conceptually, this approach moved the theory of controlled drug delivery a major step forward towards precision drug delivery. It shows great promise to be integrated into precision medicine to lower the toxicity and enhance the therapeutic efficacy in cancer treatment.

Supplementary Material

Refer to Web version on PubMed Central for supplementary material.

Acknowledgments

The authors thank the financial support from NIH/NCI (R01CA199668 & 3R01CA115483), NIH/NIBIB (5R01EB012569), NIH/NICHD (1R01HD086195) and DoD PRMRP Award (W81XWH-13-1-0490).

References

1. Marcus PM, Pashayan N, Church TR, Doria-Rose VP, Gould MK, Hubbard RA, Marrone M, Miglioretti DL, Pharoah PD, Pinsky PF, Rendle KA, Robbins HA, Roberts MC, Rolland B, Schiffman M, Tiro JA, Zauber AG, Winn DM, Khoury MJ. Cancer Epidemiol Biomarkers Prev. 2016; 25:1449–1455. [PubMed: 27507769]
2. Blau R, Krivitsky A, Epshtein Y, Satchi-Fainaro R. Drug Resist Updat. 2016; 27:39–58. [PubMed: 27449597]
3. Wu J, Qu W, Williford JM, Ren Y, Jiang X, Jiang X, Pan D, Mao HQ, Luijten E. Nanotechnology. 2017; 28:204002. [PubMed: 28266928]
4. Wang J, Mao W, Lock LL, Tang J, Sui M, Sun W, Cui H, Xu D, Shen Y. ACS Nano. 2015; 9:7195–7206. [PubMed: 26149286]
5. Quader S, Liu X, Chen Y, Peng M, Chida T, Ishii T, Miura Y, Nishiyama N, Cabral H, Kataoka K. Journal of controlled release. 2017; 258:56–66. [PubMed: 28483513]
6. Jiang X, Qu W, Pan D, Ren Y, Williford JM, Cui H, Luijten E, Mao HQ. Adv Mater. 2013; 25:227–232. [PubMed: 23055399]
7. Zhang M, Dai T, Feng N. Nanoscale Res Lett. 2017; 12:274. [PubMed: 28410552]
8. Yi H, Liu P, Sheng N, Gong P, Ma Y, Cai L. Nanoscale. 2016; 8:5985–5995. [PubMed: 26926103]
9. Zhang F, Elsabahy M, Zhang S, Lin LY, Zou J, Wooley KL. Nanoscale. 2013; 5:3220–3225. [PubMed: 23474773]
10. Deng B, Ma P, Xie Y. Nanoscale. 2015; 7:12773–12795. [PubMed: 26176593]
11. Kern HB, Srinivasan S, Convertine AJ, Hockenbery D, Press OW, Stayton PS. Molecular pharmaceutics. 2017; doi: 10.1021/acs.molpharmaceut.6b01178
12. Logie J, Ganesh AN, Aman AM, Al-Awar RS, Shoichet MS. Biomaterials. 2017; 123:39–47. [PubMed: 28161682]
13. Jena SK, Sangamwar AT. Therapeutic delivery. 2017; 8:109–111. [PubMed: 28145829]
14. Zeng Q, Li H, Jiang H, Yu J, Wang Y, Ke H, Gong T, Zhang Z, Sun X. Biomaterials. 2017; 122:105–113. [PubMed: 28110170]
15. Wang Q, Jiang H, Li Y, Chen W, Li H, Peng K, Zhang Z, Sun X. Biomaterials. 2017; 122:10–22. [PubMed: 28107661]

16. Xiao K, Luo J, Fowler WL, Li Y, Lee JS, Xing L, Cheng RH, Wang L, Lam KS. Biomaterials. 2009; 30:6006–6016. [PubMed: 19660809]
17. Xiao K, Li Y, Lee JS, Gonik AM, Dong T, Fung G, Sanchez E, Xing L, Cheng HR, Luo J, Lam KS. Cancer research. 2012; 72:2100–2110. [PubMed: 22396491]
18. Xiao K, Li YP, Wang C, Ahmad S, Vu M, Kuma K, Cheng YQ, Lam KS. Biomaterials. 2015; 67:183–193. [PubMed: 26218744]
19. Xiao K, Luo J, Li Y, Lee JS, Fung G, Lam KS. Journal of Controlled Release. 2011; 155:272–281. [PubMed: 21787818]
20. Li Y, Xiao K, Luo J, Lee J, Pan S, Lam KS. Journal of Controlled Release. 2010; 144:314–323. [PubMed: 20211210]
21. Zhang X, Li L, Li C, Zheng H, Song H, Xiong F, Qiu T, Yang J. Carbohydrate polymers. 2017; 155:407–415. [PubMed: 27702529]
22. Xin K, Li M, Lu D, Meng X, Deng J, Kong D, Ding D, Wang Z, Zhao Y. ACS applied materials & interfaces. 2017; 9:80–91. [PubMed: 27957858]
23. Mittal A, Chitkara D. Therapeutic delivery. 2016; 7:73–87. [PubMed: 26769002]
24. Li Y, Xiao K, Zhu W, Deng W, Lam KS. Adv Drug Deliv Rev. 2014; 66:58–73. [PubMed: 24060922]
25. Rodriguez-Hernandez J, Babin J, Zappone B, Lecommandoux S. Biomacromolecules. 2005; 6:2213–2220. [PubMed: 16004465]
26. Li Y, Xiao K, Luo J, Xiao W, Lee JS, Gonik AM, Kato J, Dong TA, Lam KS. Biomaterials. 2011; 32:6633–6645. [PubMed: 21658763]
27. Peiris PM, Abramowski A, McGinnity J, Doolittle E, Toy R, Gopalakrishnan R, Shah S, Bauer L, Ghaghada KB, Hoimes C, Brady-Kalnay SM, Basilion JP, Griswold MA, Karathanasis E. Cancer Res. 2015; 75:1356–1365. [PubMed: 25627979]
28. Li Y, Budamagunta MS, Luo J, Xiao W, Voss JC, Lam KS. ACS Nano. 2012; 6:9485–9495. [PubMed: 23106540]
29. Li Y, Lin TY, Luo Y, Liu Q, Xiao W, Guo W, Lac D, Zhang H, Feng C, Wachsmann-Hogiu S, Walton JH, Cherry SR, Rowland DJ, Kukis D, Pan C, Lam KS. Nat Commun. 2014; 5:4712. [PubMed: 25158161]
30. Kato J, Li Y, Xiao K, Lee JS, Luo J, Tuscano JM, O'Donnell RT, Lam KS. Mol Pharm. 2012; 9:1727–1735. [PubMed: 22530955]
31. Li Y, Xiao W, Xiao K, Berti L, Luo J, Tseng HP, Fung G, Lam KS. Angew Chem Int Ed Engl. 2012; 51:2864–2869. [PubMed: 22253091]
32. Owen SC, Chan DPY, Shoichet MS. Nano Today. 2012; 7:53–65.

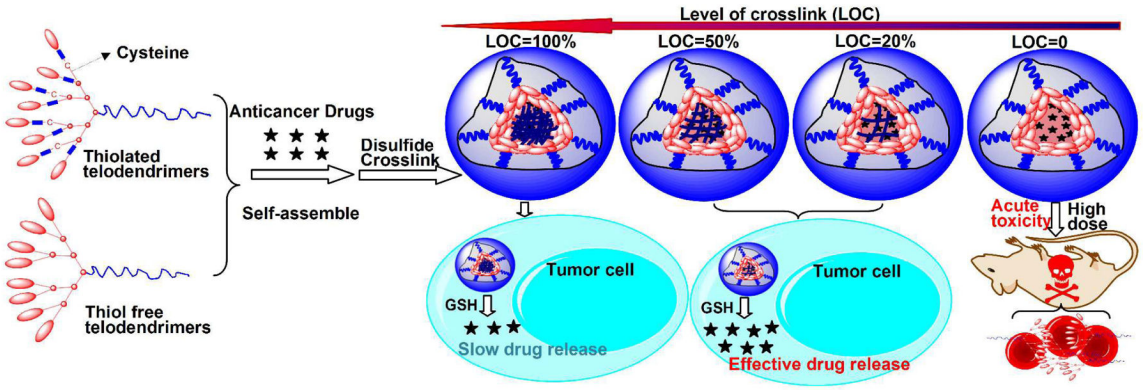

Figure 1.

Schematic illustration of the micellar nanoparticles with tunable levels of crosslink (LOC) formed by oxidization of different ratios of thiol-free telodendrimer (PEG^{5k}-CA_8) and thiolated telodendrimer (PEG^{5k}-Cys_4-L_8-CA_8) after self-assemble.

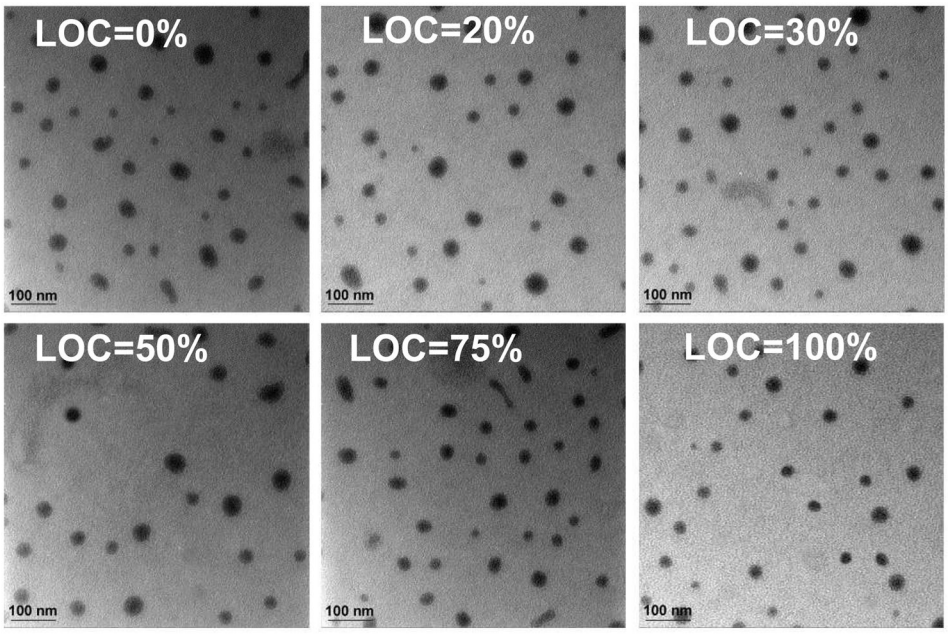

Figure 2.
TEM images of the micellar nanoparticles with tunable levels of crosslink (LOC).

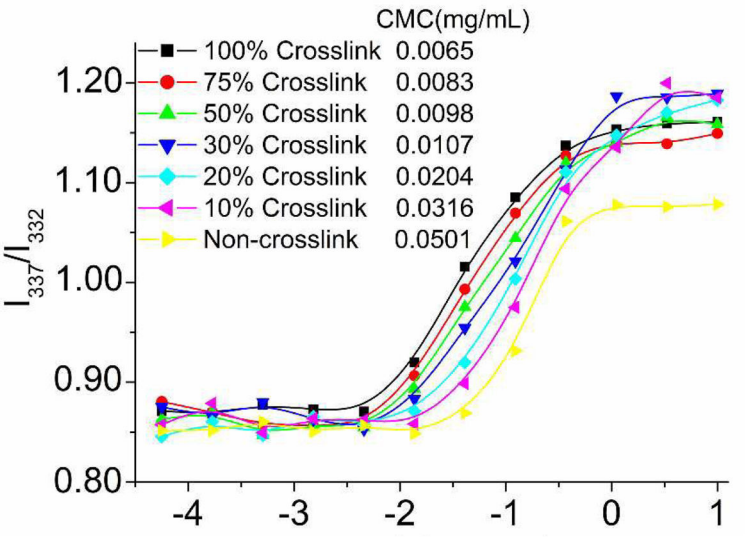

Figure 3.

Critical micelle concentrations (CMC) values of the micellar nanoparticles with different levels of crosslink (LOC) using pyrene as a probe.

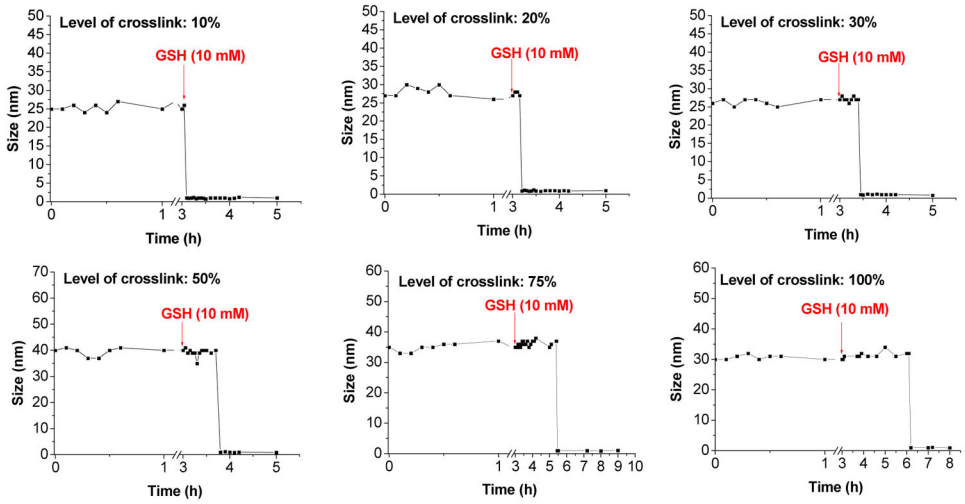

Figure 4.

Stability of the micellar nanoparticles with different levels of crosslink (LOC) (presence of particle size measured by dynamic light scattering particle sizer) as a function of LOC, in the presence of 2.5 g/L SDS and after addition of 10 mM GSH at 3 hrs. It is clear from the dissociation curves that the higher the level of the crosslink, the longer it took for the micellar nanoparticles to dissociate.

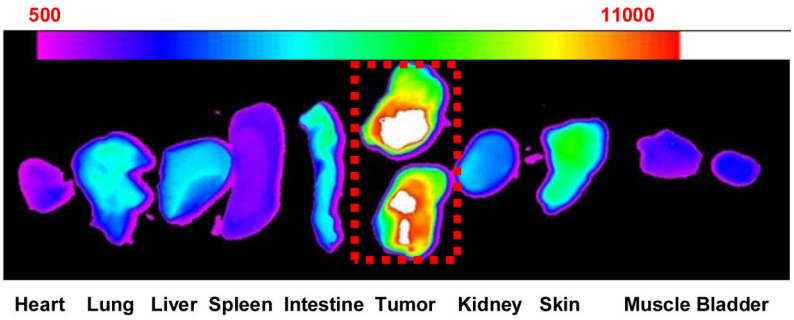

Figure 5.

Representative *ex vivo* NIRF optical images of dissected organs and tumors from nude mice bearing SKOV-3 xenograft obtained with Kodak imaging system at 24 hrs after i.v. injection of DiD and PTX co-loaded micellar nanoparticles with a LOC at **50%**; Injection volume: 100 μL, DiD: 0.5 mg/mL, PTX: 2.0 mg/mL.

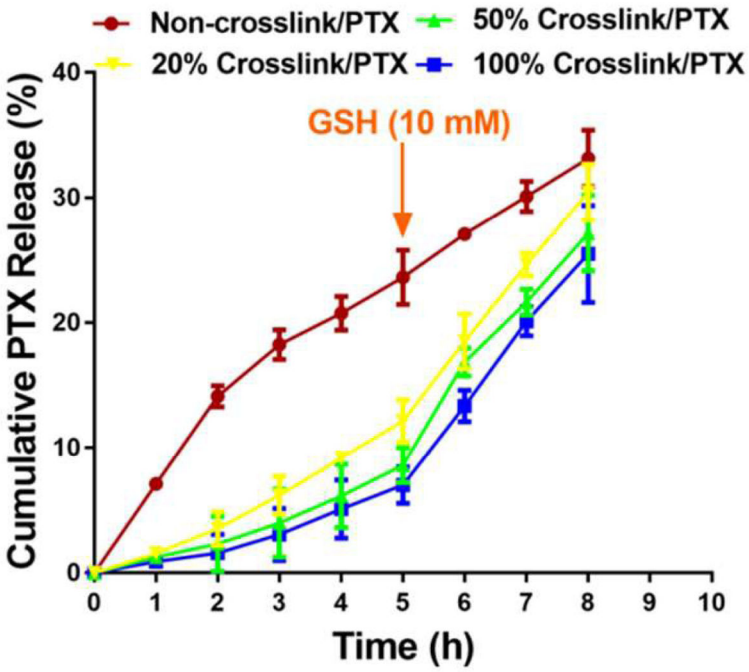

Figure 6.

Cumulative release of paclitaxel from of PTX encapsulated micellar nanoparticles with LOCs at 0%, 20%, 50% and 100% in PBS (pH 7.4) at 37°C, with triggered release at 5 hrs upon addition of 10 mM GSH.

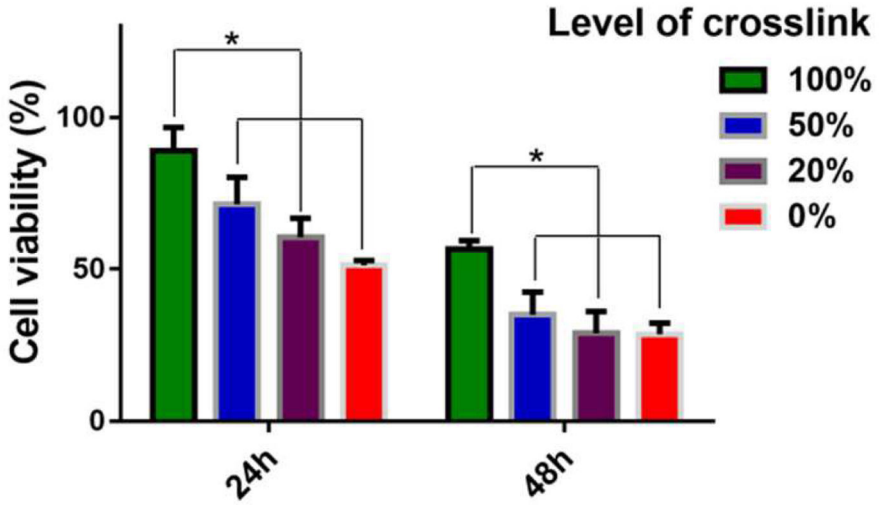

Figure 7.

MTT assays showing the viability of SKOV-3 ovarian cancer cells after 2 hrs incubation with PTX-encapsulated micellar nanoparticles with LOCs at 0%, 20%, 50% and 100%, followed by washing three times with PBS and additional 22 hrs or 46 hrs incubation (total incubation time: 24 or 48 hrs). *: $p < 0.05$. Final concentration of PTX: 13.7 ng/mL.

Table 1

The survival condition of mice treated with 200 and 400 mg/kg of the micellar nanoparticles with LOCs at 0%, 20%, 50% and 100%, respectively. (n=4)

Dose	0% crosslink	20% crosslink	50% crosslink	100% crosslink
200 mg/kg	Dead(1/4)	Alive	Alive	Alive
400 mg/kg	Dead	Alive	Alive	Alive

Table 2

The survival condition of rats treated with 200 and 400 mg/kg of the micellar nanoparticles with LOCs at 0%, 20%, 50% and 100%, respectively. (n=4)

Dose	0% crosslink	20% crosslink	50% crosslink	100% crosslink
200 mg/kg	Dead(2/4)	Alive	Alive	Alive
400 mg/kg	Dead	Alive	Alive	Alive